Biophysical Chemistry 253 (2019) 106230

Contents lists available at ScienceDirect

Biophysical Chemistry

journal homepage: www.elsevier.com/locate/biophyschem

Research Article

Incorporating phototransduction proteins in zebrafish green cone with pressure-polished patch pipettes

Marco Aquila[a,1], Daniele Dell'Orco[b], Ramona Fries[c], Karl-Wilhelm Koch[d], Giorgio Rispoli[a,*]

[a] Department of Biomedical and Specialized Surgical Sciences, Section of Physiology, Via Borsari 46, I-44121 Ferrara, Italy
[b] Department of Neurosciences, Biomedicine and Movement Sciences, Section of Biological Chemistry, University of Verona, Strada le Grazie 8, I-37124 Verona, Italy
[c] Institute of Biology and Environmental Sciences, Biochemistry Group, University of Oldenburg, Carl-von-Ossietzky-Straße 9-11, D-26111 Oldenburg, Germany
[d] Department of Neuroscience, Biochemistry Group, University of Oldenburg, Carl-von-Ossietzky-Straße 9-11, D-26111 Oldenburg, Germany

HIGHLIGHTS

- Zebrafish cones were recorded in whole-cell employing pressure-polished pipettes.
- GCAP overexpression or knock-down was performed by injecting GCAP or its antibody.
- Guanylate cyclase was already saturated with endogenous GCAP.
- The antibody slowed down photoresponse recovery and reduced light-sensitive current.
- Possibly, the antibody inhibited both the Ca^{2+}-regulated and the basal GC activity.

GRAPHICAL ABSTRACT

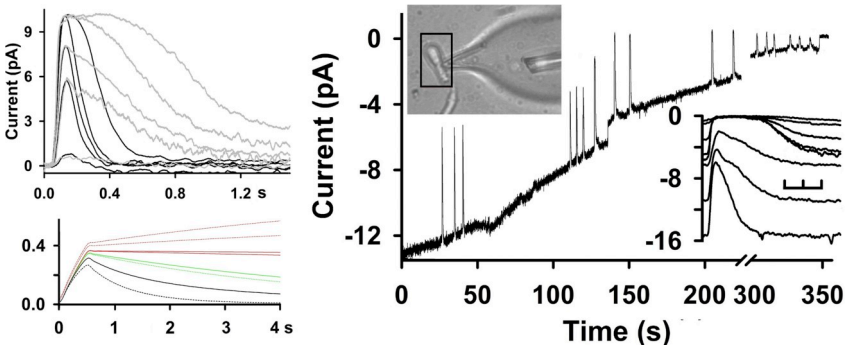

ARTICLE INFO

Keywords:
Zebrafish retina
Retinal photoreceptors
Phototransduction
Calcium signalling
Guanylate cyclase
cGMP

ABSTRACT

The neuronal Ca^{2+}-sensor guanylate cyclase-activating protein 3 (zGCAP3) is a major regulator of guanylate cyclase (GC) activity expressed in zebrafish cone cells. Here, the zGCAP3, or a monoclonal antibody directed against zGCAP3, was injected in the cone cytoplasm by employing the pressure-polished pipette technique. This technique allows to perform "real time" zGCAP3 (or of any other phototransduction protein) over-expression or knock-down, respectively, via the patch pipette. Photoresponses were not affected by purified zGCAP3, indicating that GC was already saturated with endogenous zGCAP3. The cytosolic injection of anti-zGCAP3 produced the slowing down kinetics of the flash response recovery, as theoretically expected by a minimal phototransduction model considering the antibody acting exclusively on the maximal GC activation by low Ca^{2+}. However, the antibody produced a progressive current decay toward the zero level, as if the antibody affected also the basal GC activity in the dark.

Abbreviations: Dpf, day post fertilization; GC, guanylate cyclase; PDE, cGMP phosphodiesterase; SDS-PAGE, sodium dodecylsufate polyacrylamide gel electrophoresis; HEPES, N-(2-hydroxyethyl)piperazine-N′-(2-ethanesulfonic acid); LED, light emitting diode; SPR, surface plasmon resonance; zGCAP, zebrafish guanylate cyclase-activating protein; ZG3 7E6, monoclonal antibody against; zGCAP3, absorbed photons Rh*

* Corresponding author.
E-mail address: giorgio.rispoli@unife.it (G. Rispoli).
[1] Present address: 3Brain AG, Einsiedlerstrasse 30, 8820 Wädenswil, Switzerland.

https://doi.org/10.1016/j.bpc.2019.106230
Received 26 June 2019; Received in revised form 18 July 2019; Accepted 18 July 2019
Available online 22 July 2019
0301-4622/

1. Introduction

Visual excitation and adaptation in vertebrate cone cells is much less understood than in rod cells [1]. Cones do not only mediate photopic vision, but also allow discrimination of colours and are further able to maintain their responsiveness over 6–7 orders of magnitude of background light intensities. These remarkable performances require an efficient array of signalling molecules at the subcellular level.

In recent years zebrafish has become a favourite model organism for the study of molecular processes in cone phototransduction [2]. The zebrafish retina is equipped with one type of rod cell and four types of cone cells: short single (UV-sensitive) cones, long single cones (blue-sensitive) and double cones (green- and red-sensitive). Light responses of double cones and UV-sensitive cones were measured by suction-pipette recording in response to illumination [3,4]. Progress in the genetic manipulation of zebrafish has revealed some crucial vision-related mechanisms. For example, knockdown of the cone-specific opsin kinase GRK7 has a strong effect on their photoresponse recovery, and ectopic expression of GRK7 in zebrafish rods lowered their photosensitivity [5,6]; mutations in key proteins of the phototransduction cascade lead to blindness and cone degeneration [7].

Regulation of excitation and adaptation in photoreceptor cells depends strongly on the cytoplasmic Ca^{2+} concentration and on Ca^{2+} sensor proteins like recoverin, calmodulin and the guanylate cyclase-activating proteins (GCAPs) [8,9]. Zebrafish express a set of six GCAP isoforms, of which four are exclusively transcribed in cone cells (zGCAP3, 4, 5 and 7) and transcripts of zGCAP1 and 2 are only found in rods and short single cones [10,11]. Isoforms of zGCAP differ in their Ca^{2+}-sensing and Ca^{2+}-activating properties [12]. A particular strong transcription in the larval state was observed for zGCAP3 [11], which was coincident with the onset of visual processing in the zebrafish eye and was matching protein expression profile [13]. Detailed investigations of its biochemical properties revealed that zGCAP3 is a strong activator of membrane sensory guanylate cyclases (GC), detecting and mediating Ca^{2+}-signals below 600 nM [13].

Since the photoresponse is the real-time recording of the enzymes controlling the intracellular concentration of cGMP, it is the most accurate and direct probe of the functional integrity of the entire phototransduction cascade. A key strategy to further investigate the zGCAP3 function in vivo or ex vivo, as well as of other proteins involved in phototransduction, is to study how changes in specific transduction proteins − naturally occurring or produced by site-directed artificial mutants (as well as by knock down or over-expressing mutants) − affect electrical response [14–17]. However, the production of a vital transgenic animal is often expensive and time consuming; furthermore, the protein level alteration is permanent, i.e. irreversible, and often, due to the activation of compensatory pathways, the genetic manipulation does not isolate the specific function of the protein under study [18].

On this ground, we investigated here the physiological function of zGCAP3 by measuring, in real-time, the effects on the light response of the over/down-regulation of a phototransduction protein, from a wild type (WT) condition. This has recently been made possible by the development of the pressure-polished patch pipette technique: the enlarged shank and the small tip of these pipettes allowed the recording of the light-evoked changes of photocurrent even from small photoreceptors, to accommodate pulled perfusion tubes very close to the pipette tip, and to greatly reduce the access (or series) resistance [19].

The photoresponses recorded with this technique are stable but there is a cell to cell variation regarding the response kinetics, independently by the current level and/or sensitivity, as shown also in mammalian photoreceptors [20]. This further limits the conclusions drawn from the usual knock out and overexpression experiments, because they are performed on different cells isolated from different animals, therefore a large number of recordings are required before concluding that these genetic procedures produced a genuine change of photoresponse kinetics.

Preliminary experiments were then performed to simulate the overexpression and the down-regulation of the zGCAP3, by whole-cell delivery of the protein itself or of its monoclonal antibody. Photoresponses were not affected by injection of purified zGCAP3, indicating either that GC was already saturated with endogenous zGCAP3, or that it was not the target of zGCAP3. The cytosolic injection of anti-zGCAP3 produced the expected slowing down kinetics of flash responses, but, surprisingly, the current progressively decayed toward the zero level within ~5 min of antibody perfusion. Moreover, this current fall was also observed in control experiments by injecting in the cytosol an antibody not specific for GCAP proteins, therefore these experiments must be considered cautiously to avoid erroneous conclusions. Finally, the GC activity modulation and the cell to cell variation of response recovery kinetics are also collectively analysed by using a minimal mathematical model of phototransduction.

Preliminary results have been presented in abstract form [21].

2. Materials and methods

2.1. Cone isolation and viewing

All experiments on zebrafish (*Danio rerio*) were performed in compliance with the European Communities Council Directive for animal use in science (86/609/EEC) and approved by a local ethical committee. Details of the methods are described in Ref. [19]; briefly, photoreceptors were mechanically isolated from healthy, dark-adapted zebrafish, in a fully darkened box equipped with infrared LEDs (wavelength: 940 nm) by using a high definition webcam connected to an external monitor. An aliquot (~2 ml) of the Ringer solution (composition, in mM: 115 NaCl, 3 KCl, 10 HEPES free acid [*N*-(2-hydroxyethyl) piperazine-*N′*-(2-ethanesulfonic acid)], 0.6 $MgCl_2$, 0.6 $MgSO_4$, 1.5 $CaCl_2$, 10 glucose, buffered to pH = 7.6 with NaOH; osmolality: 260 mM mOsm/kg) containing the photoreceptors was transferred to the recording chamber placed on the microscope (TE 300, Nikon, Tokyo, Japan) stage. The preparation was illuminated with a cluster of ultra-bright infrared LED (900 nm) and focused on a fast digital camera (C6790–81, Hamamatsu Photonics, Tokyo, Japan) coupled to the microscope.

2.2. Protein expression and purification

Proteins were heterologously expressed in *E. coli* and purified as described in Refs. [22–24]. Amino acid sequence alignments of the six zGCAP isoforms revealed a high degree of sequence diversity in the carboxy-terminal part making it a prime candidate region for producing zGCAP isoform specific antibodies. A peptide comprising the last 20 amino acids C-KMMDLTHVLEIIVNGQKKKKE (residues 168–188) from zebrafish zGCAP3 protein was synthesized and coupled to BSA and OVA via an additional C at the amino terminus (PSL, Heidelberg, Germany). Rats were immunized subcutaneously and intraperitoneally with a mixture of 50 μg peptide-OVA, 5 nmol CPG oligonucleotide (Tib Molbiol, Berlin, Germany), 500 μl PBS and 500 μl incomplete Freund's adjuvant. A boost without adjuvant was given six weeks after the primary injection; fusion was performed using standard procedures. Supernatants were tested in a differential ELISA with the zGCAP3 peptide coupled to BSA and irrelevant peptides coupled to the same carrier. MAbs that reacted specifically with the zGCAP3 peptide were further analysed in Western blot. A monoclonal antibody named ZG3 7E6 (rat IgG1) subclass was used in this study; another one, directed against the intracellular part of CD3, was used in controls. Monoclonal IgG antibodies were purified from hybridoma fluids by diluting IgG samples ten-fold in 20 mM Na-phosphate buffer, pH = 6.5 and loading on a cation exchange column (Fractogel EMD, CM column, Merck, Darmstadt, Germany). Bound proteins were eluted by a linear NaCl gradient from 0 to 300 mM in 20 mM Na-phosphate, pH 6.5. Fractions were

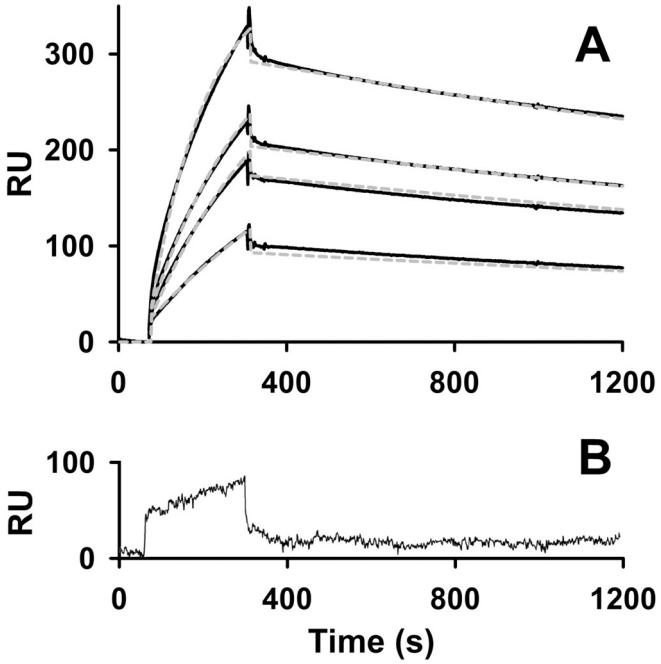

Fig. 1. (A) SPR analysis of IgG 7E6 binding to zGCAP3. In order to precisely assess the affinity of purified IgG17E6, different ZG3 7E6 concentrations (0.13 μM, 0.22 μM, 0.33 μM, 0.67 μM, and 1.34 μM) in SPR running buffer were injected over zGCAP3 protein (immobilized at 2 ng/mm^2 on the CM5 sensor chip) at 10 μl/min for 4 min. Grey dotted lines results from global fitting analysis, which gave: $k_{on} = 2.57{\cdot}10^4\,M^{-1}\,s^{-1}$, $k_{off} = 2.58{\cdot}10^{-4}\,s^{-1}$, and $K_D = k_{off}/k_{on} = 10$ nM ($\chi^2 = 14.6$). (B) Control recording with 0.27 μM ZG3 7E6 applied over immobilized zGCAP4 (4.5 ng/mm^2).

collected and checked for purity and immunoreactivity by SDS-PAGE, immunoblotting and surface plasmon resonance (SPR) spectroscopy (Fig. 1). SPR was employed to screen of anti-zGCAP3 positive hybridoma fluids for testing of specificity and sufficient affinity, and to determine the kinetics and affinity constants. Initial testing of hybridoma fluids by immunoblotting revealed no cross-reactivity of anti-zGCAP3 antibodies to other zGCAP isoforms. To select among the different IgGs for further purification and processing we immobilized zGCAP3 and zGCAP4 (control) by amine-coupling on CM5 sensor chips (2 ng/mm^2) and supplied IgG samples in SPR running buffer (150 mM NaCl, 3 mM EDTA, 10 mM HEPES-KOH pH 7.4). ZG3 7E6 showed the lowest degree of dissociation indicating a rather high affinity. It was therefore further purified by cation exchange chromatography (see Methods) to remove non IgG protein from the solution.

Affinity of purified ZG3 7E6 was finally tested by injecting different concentrations of ZG3 7E6 in running buffer and recording of sensorgrams, which were evaluated with the BIAevaluation software 4.1. A purified monoclonal antibody, named ZG3 7E6, was chosen for its high specificity for zGCAP3 and lack of cross-reaction with other GCAP isoforms (Fig. 1). The affinity of ZG3 7E6 for zGCAP3 was measured with SPR: the latter protein was immobilized on a SPR sensorchip surface, while the former was injected at different concentrations into the flow cell. The K_D yielded by the global fitting analysis to the sensorgrams obtained with increasing ZG3 7E6 concentrations was 10 nM (Fig. 1A), while its average value for 34 single sensorgrams was 12 ± 0.3 nM. Presence or absence of Ca^{2+} in the SPR running buffer did not influence the interaction between zGCAP3 and ZG3 7E6, nor changing the running buffer to the zebrafish intracellular cone solution used in the electrophysiological recordings (K_D became ~14 nM). A control recording of ZG3 7E6 flushed over immobilized zGCAP4 showed no specific binding signal (Fig. 1B).

2.3. Recordings from zebrafish cones, light stimuli and intracellular perfusion

Light responses of zebrafish cones were recorded using the whole-cell configuration of the patch-clamp technique, under dark-adapted condition at room temperature (20–22 °C); details of the patch-clamp apparatus are described in Refs. [19,25,26].

Patch pipettes were filled with an intracellular solution containing (in mM): 40 KCl, 70 K-Asp, 5 $MgCl_2$, 1 GTP, 5 ATP, 5 HEPES (buffered to pH = 7.6 with KOH; osmolality: 260 mM mOsm/Kg). The intracellular dialysis of zebrafish cones was performed by using pressure-polished pipette and an intrapipette perfusion system. The enlarged shank of pressure-polished pipette besides improving the electrical recordings, allows to accommodate pulled quartz or plastic perfusion tubes close to the pipette tip (Fig. 3 inset, right), allowing the fast and controlled cytosolic incorporation of exogenous molecules [19,25,26]. Perfusion tube was filled with ZGCAP3 or its specific antibody, dissolved in the intracellular solution at a concentration of 40 μM and 6 μM, respectively. The protein solution was injected in the cytosol during whole-cell recording by the controlled application of pressure to the capillary lumen, delivered by a commercially available perfusion pressure/vacuum generator (2PK+, ALA scientific instruments, New York, New York; applied pressure: ~40 PSI (~280 kPa)), or with a 1 ml precision syringe coupled to a micromanipulator. Successful perfusion of the protein solution was checked by injecting lucifer yellow [19] or 20 μM of dansyl chloride-labeled zGCAP3 (degree of dansylation: 16–22%; Fig. 3 inset, left) once the whole-cell recording was gained. Incorporation of fluorescent zGCAP3 into the zebrafish cone cytosol was rapid and sufficient to measure possible modifications of the photoresponse waveform induced by application of either purified zGCAP3 or an anti-zGCAP3 antibody.

Light stimuli were designed using the voltage protocols of Clampex software: the analogical outputs of the Digidata board drove a calibrated voltage-to-current converter connected to an ultra-bright trichromatic LED (with centre wavelength red/green/blue of 627.5 ± 8/525 ± 10/467.5 ± 8 nm), coupled to the binocular port of the inverted microscope (Nikon TE-300, Tokyo, Japan). The LED was aligned as described in Refs. [19], so to have its light spot automatically centred and in focus on the zebrafish cone, when the latter was viewed in sharp focus through a 60× objective on the microscope camera.

Responses were analysed with Clampfit (Molecular Devices) and Sigmaplot (Systat Software Inc., San Jose, CA, USA) software; mathematical simulations were performed with Mathcad (Parametric Technology Corporation, Needham, MA, USA) software. To reject as much noise as possible, each photoresponse shown in the figures was the average of three or more responses to the same flash; this average response was then further filtered by using a local smoothing routine implemented in the commercially available program Sigmaplot. The routine parameters were set to obtain low-pass filtering of 30 Hz (negative exponential was selected for smoother function, with a sampling proportion of 0.01, a polynomial degree 1, and a number of interval that was 1/10 of the total number of samples constituting each trace, i.e. 19,220 samples for a 1 s trace) [19].

Results are given as means ± SEM; all chemicals were purchased from Sigma (St. Louis, MO, USA).

3. Results

3.1. Response waveform

Long lasting (> 20 min) whole-cell recordings from the very small and fragile zebrafish cones were obtained with patch pipette with a very small tip and an enlarged shank [19]. This particular shape allows low access resistance recordings and permits to accommodate a perfusion tubes very close to the pipette tip (Fig. 3 inset, right). In this way, exogenous molecules were efficiently delivered in the cell cytosol

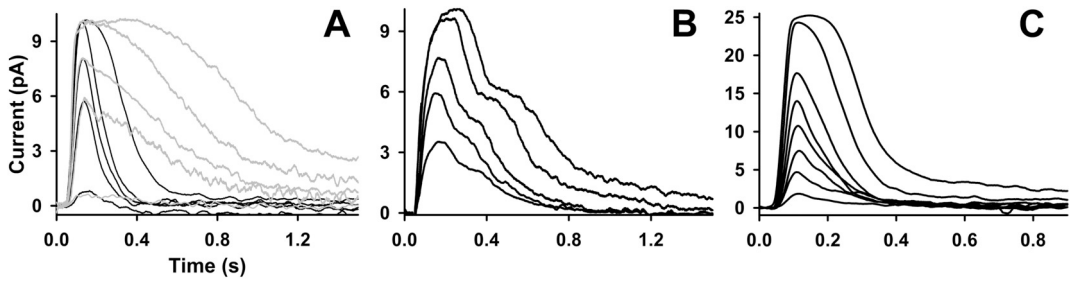

Fig. 2. Different flash response waveforms. Each trace is the average to 3 responses but the one corresponding to the dimmest flash ($1.14{\cdot}10^2$ photons/μm^2), that is the average of 9 (A) and 12 (C) responses; the average traces were then smoothed as described in the methods, aligned with the flash timing (flash delivered at 0 time), and plotted with the same time-scale. (A) Dark traces, responses to 1 ms flashes of intensity $1.14{\cdot}10^2$, $2.32{\cdot}10^3$, $4.49{\cdot}10^3$, $8.68{\cdot}10^3$, $1.77{\cdot}10^4$ photons/μm^2; grey traces, responses of another green cone with a slower kinetics to the same flash intensities. (B) Responses of a green cone exhibiting a two-phase recovery to 1 ms flashes of intensity: $1.14{\cdot}10^3$, $2.32{\cdot}10^3$, $4.49{\cdot}10^3$, $8.68{\cdot}10^3$, $1.77{\cdot}10^4$ photons/μm^2. (C) Responses of a fourth cone, exhibiting a very large current and monotonic recovery, to flashes of intensity $1.14{\cdot}10^2$, $2.28{\cdot}10^2$, $4.56{\cdot}10^2$, $2.32{\cdot}10^3$, $4.49{\cdot}10^3$, $8.68{\cdot}10^3$, $1.77{\cdot}10^4$ photons/μm^2.

through the patch pipette. We narrowed our research to green cones because they can be isolated from the zebrafish retina in larger numbers than the other cone types; the trichromatic LED was used to ensure that the cone was indeed green-sensitive. Light flashes of increasing intensity (range: $1.14{\cdot}10^2 \div 3.76{\cdot}10^6$ photons/μm^2) were delivered, in triplets in repeated sequences, in the dark or on a background of light (range: $1.3{\cdot}10^4 \div 2.6{\cdot}10^5$ photons/(μm$^2{\cdot}$s). Very dim flashes, to check the threshold sensitivity (that was $1.14{\cdot}10^2$ photons/μm^2), were repeated at least 9 times to have a reliable waveform. Recordings were remarkable stable, with negligible changes in sensitivity, light adaptation properties and response kinetics within at least 10 min of recording, during which it was possible to deliver no < 50 light flashes.

Averaged and smoothed responses to the same flash intensity exhibited slow or fast kinetics (Fig. 2), with a monotonic (Fig. 2A) or, in about 40% of the recordings, a biphasic (Fig. 2B) recovery phase. The latter was particularly evident for flash intensities in the range $2{\cdot}10^3 \div 10^4$ photons/μm^2: dim flashes or supersaturating flashes elicited always monotonic responses. The different kinetics and waveform are probably generated by the cell to cell variability of the cytosolic Ca^{2+} buffering capacity [19], but not by the different light sensitivity or current amplitude (that varied between 8 and 30 pA; average: 18.4 ± 1.9 pA, $n = 32$), that were similar in the three cones (selected among the 32 ones examined here) shown in Fig. 2A and B. However, when current exceeded 20 pA, the response recovery phase was always monotonic Fig. 2C). Theoretical considerations (see Discussion), based on a simple model, showed indeed that the response kinetics is independent by the sensitivity, slightly accelerated as the current increases, and strongly accelerated by accelerating the basal activity in the dark of GC (and of phosphodiesterase, PDE).

3.2. Manipulating single cone cells of adult zebrafish

To test the feasibility of the intracellular protein delivery during whole-cell recordings, it was analysed the effect on the zebrafish cone photoresponse of cytosolic injection of either exogenous zGCAP3 or its specific monoclonal antibody (to simulate the overexpression or down-regulation, respectively, of zGCAP3 in adult WT zebrafish cone). The effectiveness of the molecular cytosolic loading was checked by measuring the diffusion into the cell from the pipette of fluorescence dyes, as lucifer yellow (Ref. [19]) or dansylated zGCAP3 (Fig. 3 inset). Next step was to test the effect of the exogenous protein. Photoresponses from very dim (to check the photoreceptor sensitivity) up to saturating flashes (to measure the dark current amplitude) were collected over few minutes, to ensure the response reproducibility and cell healthiness over the time. After these control experiments, proteins were injected applying a positive pressure to the pipette perfusion tube for ~10 s, and the same light stimuli protocol used in control was repeated. If no effect was observed, the injection was repeated over and over again up to

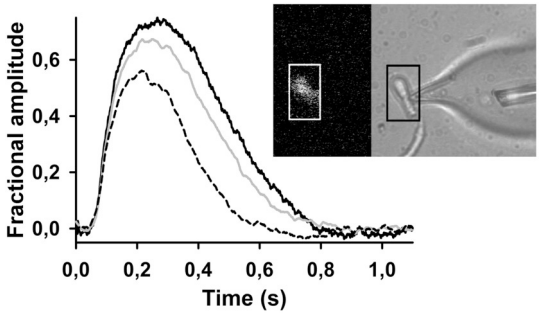

Fig. 3. Intracellular delivery of zGCAP3 into a zebrafish cone. Effect of zGCAP3 delivery on a zebrafish cone photoresponse; each one of the three traces are the average of three consecutive responses to the same flash ($4.49{\cdot}10^3$ photons/μm^2) before (black trace), during (dashed trace) and after (grey trace) the application of 40 μM of purified zGCAP3 (dissolved in the intracellular solution; average dark current of the entire recording is 5.7 pA). (Inset) Microphotograph of the pipette and of a cone cell shown in fluorescence (left) and in bright field (right) following the injection of 20 μM of dansyl chloride-labeled zGCAP3 through the perfusion tube (visible on the right; pipette fluorescence was digitally subtracted from the image on the left); the rectangle encloses the cone cell in both panels, its longer side is 20 μm.

expel a volume of solution containing the protein (~80 μl) that was at least three times the volume of the control solution filling the patch pipette (i.e. ~25 μl).

It was tested first purified recombinant zGCAP3, having high sensitivity to Ca^{2+} in the sub-micromolar range and strong activation of sensory GCs, being half-maximal at Ca^{2+} concentrations of ~30 nM [13]. Since it has been estimated that mammalian GCAP1 and GCAP2 have a concentration in the lower micromolar range [27]), the zGCAP3 was then perfused to a concentration of 40 μM, that was even above the value of 33 μM determined in carp cones [28]. However, the cytosolic perfusion of 40 μM of zGCAP3 (dissolved in the intracellular solution, see Methods) did not alter significantly the photoresponse waveform of green sensitive cones ($n = 7$; data not shown). In only two cells that had an unusual small dark current amplitude and slow flash response waveform, the application of zGCAP3 produced a slight falling phase acceleration and an amplitude reduction of the flash response, that was substantially reversible (Fig. 3); moreover, the dark current did not change as the response accelerated.

To perform the real-time down-regulation of zGCAP3, it was intracellularly delivered the antibody ZG3 7E6, able to interfere with the protein binding sites for Ca^{2+} and/or for the GC.

The cytosolic injection of ZG3 7E6 antibody (6.7 μM) produced the progressive slow-down of the recovery phase of the flash response (Fig. 1B). This result is expected, since the Ca^{2+} sensitivity of GC should be progressively reduced as the antibody accumulates in the cytosol.

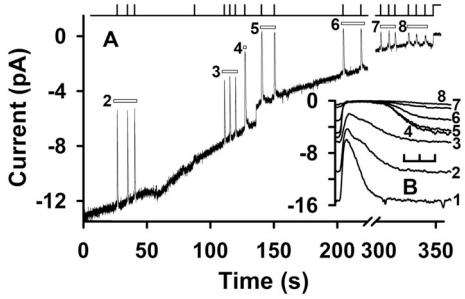

Fig. 4. Intracellular delivery of the monoclonal antibody ZG3 7E6 into a zebrafish cone. (A) Recording on a slow time scale of the dark current during the application (that begun before time 0) of 6.7 μM of purified ZG3 7E6 dissolved in the intracellular solution; flashes of a $6.07{\cdot}10^3$ and a $9.39{\cdot}10^4$ photons/μm^2 of intensity were delivered during the current fall; a step of light of $1.9{\cdot}10^7$ photons/(μm^2·s) was delivered at the end of recording to check the residual dark current. (B) Average of three non-saturating responses to a $6.07{\cdot}10^3$ photons/μm^2 flash (to check the response waveform) delivered at the beginning of recording (trace 1, not shown in (A)), at ~35 s in (A) (trace 2, responses averaged indicated by corresponding bar 2 in (A)), and at ~115 s (trace and bar 3); oversaturating responses to $9.39{\cdot}10^4$ photons/μm^2 (to check the zero light-sensitive current) at ~127 s (trace and bar 4, single response), ~145 s (trace and bar 5, two responses averaged), ~212 s (trace and bar 6, two responses averaged), ~310 s (trace and bar 7, three responses averaged), and ~332 s (trace and bar 8, three responses averaged); all responses were aligned to the zero dark current. The horizontal bar in (B) is the 0.4 s long.

Unexpectedly, the light sensitive current decayed irreversibly toward zero, since there was a progressive fall of saturating flash response amplitude, with no changes in the zero level of dark current ($n = 6$, Fig. 4). Regretfully, but anyway important to report for a methodological point of view, the current decay and a slight slow-down of the flash response were observed with a control antibody (anti-CD3), which did not react with GCAPs.

3.3. Theoretical interpretation of the results

To isolate the contribution of the GC/GCAP complex in the response recovery, and to investigate how the latter is affected by the overexpression or knock out of the Ca^{2+}-feedback mediated by the GC/GCAP complex, we developed a very simplified mathematical model. We restrict the model to a few variables, since most molecular parameters of zebrafish cone phototransduction are largely unknown. Following the reasoning described in Ref. [29], the intracellular cGMP change with time $cG(t)$ can be described by:

$$\frac{dcG(t)}{dt} = \alpha(t) - \beta(t) \bullet cG(t)$$

where $\alpha(t)$ is the change of GC activity with time, where its Ca^{2+} dependency is not developed yet, and $\beta(t)$ is PDE activity, which implicitly contains the light stimulus. The current amplitude $i(t)$, the fractional suppression of current of a flash delivered in the dark $R(t)$ or on a background of light $R_{BKG}(t)$, when the cGMP concentration reached a steady state level cG_{BKG}, can be described by:

$$i(t) = K_1 \bullet cG(t)^n;\ R(t) = 1 - \frac{cG(t)^n}{cG_d{}^n};\ R_{BKG}(t) = 1 - \frac{cG(t)^n}{cG_{BKG}{}^n}.$$

To the aim of this discussion, it is not important to model the activation phase of the response, and simply consider the activation as instantaneous, i.e. it is just a dimensionless constant factor C_β (expressing the gain of the phototransduction cascade) of the light stimulus $\phi(t)$, expressed in isomerizations/s (Rh*/s). C_β was calculated so to have a similar sensitivity of the green cones recorded here, assuming a collecting area of 1 μm^2 [19]. If the GC has a constant activity in the dark α_d and it is assumed that it does not change with Ca^{2+}, then the intracellular cGMP change with time is simply described by:

$$\frac{dcG(t)}{dt} = \alpha_d - [\beta_d + C_\beta \bullet \phi(t)] \bullet cG(t) \quad (1)$$

where β_d is the basal activity of PDE in the dark:

$$\beta_d = \frac{\alpha_d}{cG_d}$$

being cG_d the cGMP concentration in the dark, generating a current of amplitude i_d:

$$i_d = K_1 \bullet cG_d{}^n$$

For simplicity, if the light stimulus $\phi(t)$ is delivered at $t = 0$, then $\phi(0) = 0$ and $cG(0) = cG_d$. At minimum, even neglecting the Ca^{2+} buffering capacity of the cell, the Ca^{2+} regulation of GC requires to know the fraction of $i(t)$ carried by Ca^{2+}, the rate of extrusion of Ca^{2+} by the exchanger and how Ca^{2+} regulates GC. Because of high exchanger activity and strong Ca^{2+} buffering [29], the photoreceptor cytoplasm can be regarded as a well-stirred compartment [30,31], i.e. the longitudinal Ca^{2+} distribution mirrors the cGMP one. Therefore, the cGMP changes produced by the GC could be described by a steady state component in the dark α_d, summed to a component that is cooperatively regulated [32] by Ca^{2+} (i.e. by cGMP), as follows:

$$\frac{dcG(t)}{dt} = \alpha_d + A_{max} \bullet \frac{[cG_d - cG(t)]^m}{K_2 + [cG_d - cG(t)]^m}$$

where m is the cooperativity index, K_2 describe how sensitive is the GC activity to a decrease of cGMP (i.e. of Ca^{2+}), and A_{max} is proportional to the maximal rate of cGMP synthesis $\frac{dcG(t)_{max}}{dt}$ in the presence of saturating light stimuli (i.e. when $cG(t) = 0$), that is:

$$\frac{dcG(t)_{max}}{dt} = \alpha_d + A_{max} \bullet \frac{(cG_d)^m}{K_2 + (cG_d)^m}$$

Finally, the equation describing the cGMP changes is the solution of the following differential equation:

$$\frac{dcG(t)}{dt} = A_{max} \bullet \frac{[cG_d - cG(t)]^m}{K_2 + [cG_d - cG(t)]^m} + \alpha_d - \left[\frac{\alpha_d}{cG_d} + C_\beta \bullet \phi(t)\right] \bullet cG(t) \quad (2)$$

The values of all parameters reported in Fig. 5 legend were chosen according to the literature (discussed in Ref. [29]). Despite the simplicity of the model, it accounts for the expected features of the light response, i.e. that the response recovery is faster if the GC is regulated by the Ca^{2+} reduction during the light stimulation (Fig. 5A), and this acceleration is particularly large for stronger flashes; the response is desensitized and accelerated on a background of light, and this acceleration is further enhanced when GC is regulated (Fig. 5B and C). Independently by the GC regulation, the response recovery is not affected by the light sensitivity (C_β), slightly accelerate as the dark current increases (cG_d; Fig. 5D) and accelerated by increasing the basal activity in the dark of GC (α_d; Fig. 5E), which is also the cGMP turnover rate in the dark or the dark PDE activity. The knock down or the overexpression of the GC regulation by GCAP slowed down or accelerated the flash response (Fig. 6), respectively, but it did not affect the dark current level, as found here (Fig. 3) for overexpression and by others for knock down (discussed below). However, we found that the GCAP knock down with the antibody, besides the expected slowing down of the response, decreased the dark current as well. This could be explained by assuming that the antibody, besides blocking substantially the Ca^{2+} regulation of the GC by an amount $I_1 \leq 1$, it blocks also its basal activity α_d by an amount $I_2 \leq 1$, as follows:

$$\frac{dcG(t)}{dt} = A_{max} \bullet I_1 \bullet \frac{[cG_d - cG(t)]^m}{K_2 + [cG_d - cG(t)]^m} + \alpha_d \bullet I_2 - \left[\frac{\alpha_d \bullet I_2}{cG_d} + C_\beta \bullet \phi(t)\right] \bullet cG(t) \quad (3)$$

The blockade of the Ca^{2+}-regulation only of GC (i.e. $I_1 \ll 1$, $I_2 = 1$), produces a slow-down of the flash response (delivered in the dark or on

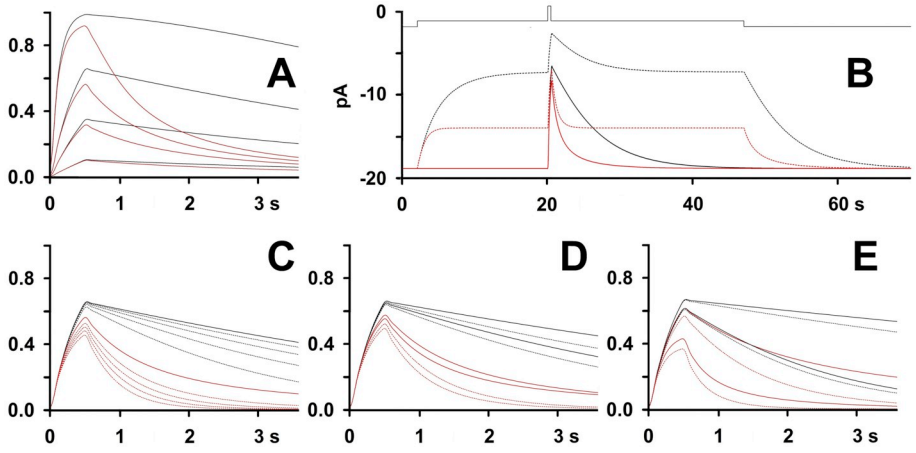

Fig. 5. Theoretical prediction of the effect of cGMP homeostasis on photoresponse. In all panels are plotted the flash response in the dark (solid traces) on a background of light (dotted traces), in the absence (black traces; Eq. (1)) or in the presence of the Ca^{2+} regulation of GC (red traces; Eq. (2)). The flash responses of panel (A), (C), (D) and (E) are expressed as fractional suppression of the current $R(t)$ or $R_{BKG}(t)$, aligned at 0 time and at 0 current. All parameters, unless specified otherwise, are: $A_{max}=10\,\mu M/s$; $K_1 = -0.15$ pA/(μM)^3; $K_2 = 3\,\mu M$; $m = 2$; $n = 3$; $\alpha_d=1\,\mu M/s$; $C_\beta=3{\cdot}10^{-4}$; $cG_d=5\,\mu M$, giving a current amplitude of 18.75 pA. (A) Response to flashes of intensity $1.25{\cdot}10^2$, 10^3, $1.25{\cdot}10^3$, 10^4 Rh*. (B) 70 s long simulation of a flash response of intensity 10^3 Rh*, delivered after 20 s of the simulation beginning in the dark and on a background of light, turned on after 2 s and lasting 45 s, of intensity of 250 Rh*/s (background and flash timing is above); same parameters of (A). (C) Response to a flash of intensity $1.25{\cdot}10^3$ Rh* delivered in the dark and on a background of 100, 250, 500, 1000 Rh*/s. (D) effect of the cGMP concentration (cG_d) on the flash response recovery in the dark and on a background of light (light stimuli as in (B)): slower traces: $cG_d = 3.5\,\mu M$, giving a current amplitude of 6.43 pA (the smallest ever recorded); faster traces: $cG_d = 6\,\mu M$, giving a current amplitude of 32.4 pA (larger than the largest current ever recorded). (E), effect of the cGMP flux (α_d) on the flash response recovery: slowest traces: $\alpha_d = 0.5\,\mu M/s$; faster traces: $\alpha_d=3\,\mu M/s$. (For interpretation of the references to colour in this figure legend, the reader is referred to the web version of this article.)

a background of light) and makes the responses of the light step larger; the blockade of both the Ca^{2+}-regulation and the basal activity in the dark of GC (i.e. I_1, $I_2 \ll 1$) produces a large decay of current as soon as the light is delivered (Fig. 6), although the background of light is kept dimmer and shorter than in the simulations of Fig. 5.

4. Discussion

4.1. Response kinetics

An interesting feature of the flash response waveform, not carefully examined in the literature, is the cell to cell difference of its kinetics and recovery phase (slow, fast, monotonic or biphasic). The biphasic recovery occurs when the transient intracellular Ca^{2+} fall elicited by the flash is significant, but at the same time the flash intensity is low enough to allow the cascade (i.e. the PDE) to be quickly inactivated. Moreover, in the presence of very large currents the response recovery was always monotonic (Fig. 2C). As discussed in Ref. [19], the difference between the two recovery phases originates by a different intracellular Ca^{2+} dynamics, which in fact regulates a plethora of Ca^{2+} sensor proteins regulating the phototransduction cascade at various levels (as GC, Rhodopsin Kinase, cGMP channel, etc.), collectively acting as a negative feedback. It is possible to mathematically demonstrate that the difference between monophasic and biphasic response may simply due to a different cell buffering capacity for Ca^{2+}, that act as a delay in the branch of the Ca^{2+}-dependent negative feedback regulating the light response [19]. Therefore, the current being equal, the cell with a slow recovery kinetics and/or a slow biphasic recovery is thought to have a larger buffering capacity (i.e. a larger delay in the feedback branch) than a cell exhibiting a fast monotonic response; if the current is very large, the buffer is then always close to be saturated by Ca^{2+} during the photoresponse and the recovery is fast and monotonic (Fig. 2C).

Besides the action of the buffer in governing the response recovery, a minimal model of phototransduction shows that the basal activity of GC, compensated by an equal basal activity of PDE, is not enough to account for the fast recovery of the flash response in the dark (Fig. 5A) or on a background of light (Fig. 5B,C), independently by the cGMP concentration in the dark (Fig. 5D), unless it is assumed that this basal activity is very large (Fig. 5E). However, the latter condition would give an unnecessary energy expenditure, would not predict the progressive desensitization and acceleration of recovery kinetics of the flash response on a background of light of progressively increasing intensity (Fig. 5B,C), and would give poor detection of the dim light stimuli by the second order retinal neurons. Indeed, a large GC basal activity would give a too small amplitude and a too fast recovery of the dim flash responses to activate significantly the synaptic transmission machinery. Alternatively, in the absence of GC regulation and a reasonable level of GC basal activity (in the range of 1 μM/s), even if the PDE is instantaneously turned off as the light stimulation is terminated, and there is no buffer that could slow down the response recovery, it is necessary that GC is strongly activated by a reduction of intracellular cGMP (or Ca^{2+}) to account for the observed fast recovery (Figs. 5, 6). The blockade of Ca^{2+} regulation of GC by the intracellular delivery of a zGCAP antibody gave the expected slowdown of the flash response (Fig. 4), that is theoretically predicted as well (Figs. 5, 6). The model predicted no change in the dark current level, if the antibody is supposed to block the Ca^{2+} regulated activity of GC only (Fig. 5). The antibody progressively reduced instead the dark current level, and this could be explained by assuming that the antibody blocked both the

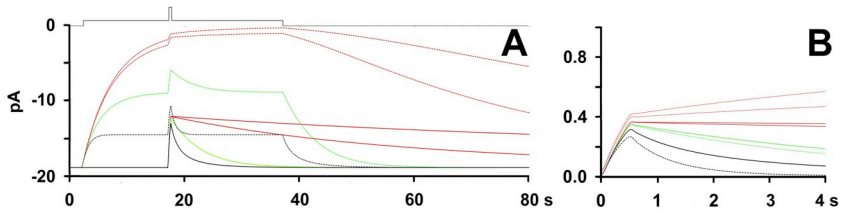

Fig. 6. Theoretical prediction of the effect of GC blockade (or overexpression). 80 s long simulation of a flash response of intensity 10^3 Rh* delivered, after 17 s of the simulation beginning, in the dark (solid traces) and on a background of light (dotted traces) turned on after 2 s and lasting 35 s, of intensity of 200 Rh*/s (top trace, background and flash timing) in control (i.e. no GC blockade, black traces), in the presence of a 100-fold reduction of the Ca^{2+}-dependent only of GC activity ($I_1 = 0.01$; $I_2 = 1$ green traces; Eq. (3)), of a 100-fold reduction of both Ca^{2+}-dependent and basal activity of GC ($I_1 = I_2 = 0.01$; red traces with almost no recovery) and in the presence of a 10-fold smaller blockade of the basal activity in respect to the Ca^{2+}-dependent one ($I_1 = 0.01$, $I_2 = 0.1$; red traces with a very slow recovery); same parameters of Fig. 5. (B) Fractional suppression of the current $R(t)$ or $R_{BKG}(t)$, of all the flash responses of (A), aligned at 0 time and at 0 current. (For interpretation of the references to colour in this figure legend, the reader is referred to the web version of this article.)

Ca^{2+} regulated and the basal GC activity (Fig. 6). However, the result that the control antibody reduced the current (although to a lesser amount) suggests that the blockade could be also a non-specific effect of the antibody on the basal activity of GC or on one or more enzymes affecting directly or indirectly the cGMP concentration, or even a non-specific blockade of the cGMP channels.

4.2. Photoresponse regulation by zGCAP3

Remarkably, zebrafish cone cells express six different GCAP isoforms that are expected to regulate three different sensory GCs [10,32,33]. We chose to explore the physiological function of zGCAP3 for several reasons: its transcripts were detected already at 3 days post fertilization (dpf) in the developing retina, coinciding with the onset of visual function [34]. Expression of zGCAP3 at the protein level was first visible at 3.25 dpf and became stronger in the following days [13]. Biochemical studies showed that zGCAP3 is a strong activator of membrane GCs exhibiting a high sensitivity for Ca^{2+}, which makes it a premium candidate to test for its physiological role [12,13]. However, using the morpholino antisense technique to knock down the expression of the zGCAP3, the optokinetic and optomotor responses of the morphants at 5–6 dpf were indistinguishable from the WT and control recordings [22]. It is therefore possible that zGCAP3 does not regulate GC at this larval stage in situ, or either its physiological function is compensated by other zGCAP isoforms. To search an answer also to these questions, the zGCAP3 and the monoclonal antibody ZG3 7E6 against it were delivered into the cytosol of isolated cone cells of adult WT zebrafish via the pressure-polished pipette, while recording the photoresponses. Perfusion of zGCAP3 did not alter significantly the photoresponse in healthy cells, although its concentration was 40 μM, i.e. comparable or even higher in respect to its endogenous concentration (see Methods). Thus, lack of any zGCAP3 effect during perfusion indicates that the GC in double cone cells (most likely the isoform zGC3 [11]) was already saturated under our measuring conditions, which is consistent with previous in vitro data on the half-maximal activation of GCs by zGCAP3 being at 0.7 μM [12]. Further, no displacement of another zGCAP seemed to occur, which could have caused a disturbance of the normal photoresponse.

The zGCAP3 regulation of endogenous GC was further explored by delivering the anti-zGCAP3 monoclonal antibody ZG3 7E6 into the green cone cell cytosol. As supported by surface plasmon resonance spectroscopy, the antibody had a very high affinity and specificity for zGCAP3, leading to a stable formation of an antigen-antibody complex (Fig. 1A). The k_{off} determined by SPR corresponds to a $1/k_{off}$ of ~65 min, therefore the antibody-antigen complex did not dissociate over the time course of a typical perfusion experiment. The decrease of the cone outer segment dark current to zero, and the progressive slowdown of the photoresponse waveform, could have mirrored a rapid shutdown of cGMP production. Although the anti-zGCAP3 antibody proved to be highly specific in western blot and SPR experiments, it accumulated in the small volume of the cone cell and could therefore have also caused non-specific disturbances, in particular during longer perfusion. Such a disturbance was for example observed with the control antibody anti-CD3. Further, the shutdown of the dark current was also surprising, because it did not match previous recordings of rod and cone dark currents of transgenic mice lacking GCAP1 and GCAP2, in which the dark current remains near normal [34–36]. It is also possible that the anti-zGCAP3 antibody had caused only a partial reduction of cGMP synthesis (at the beginning of the perfusion), but the complete shutdown of the dark current was caused by a non-specific disturbance of photoreceptor physiology. Finally, differences in recordings on mice and zebrafish photoreceptor cells might reflect differences of the cytoplasmic Ca^{2+}-concentration in the dark, which is ~250 nM in mice rods [37] and was suggested to be ~400 nM in zebrafish cones [3]. At 400 nM zGCAP3 is in its Ca^{2+}-loaded form (halfmaximal activation of GC at 30 nM Ca^{2+}; macroscopic K_D = 190 nM [12]) and mainly inactive. Although precise values on the decrease in cytoplasmic Ca^{2+} after illumination are lacking for zebrafish cones, zGCAP3 is expected to activate GC at rather low Ca^{2+}-concentrations (i.e. after high light flash intensities or sustained background illumination). Since these ambient light conditions trigger a strong activation of the PDE, an even minor disturbance of the zGCAP3-GC complex would lead to an imbalance of the cGMP homeostasis and could cause a severe reduction in the photocurrent.

Acknowledgments

Technical assistance by Andrea Margutti is gratefully acknowledged. We thank Dr. Elizabeth Kremmer for providing the monoclonal antibodies and Jeffrey Gordon (St. Louis) for providing a plasmid containing NMT from yeast *S. cerevisiae*. Financial support to G.R. included grants from the Project FAR (Fondo di Ateneo per la Ricerca) 2016-2018 and the Project FIR (Fondi per l'Incentivazione della Ricerca) 2016 of the University of Ferrara.

Declaration of Competing Interests

None.

References

[1] S. Kawamura, S. Tachibanaki, Explaining the functional differences of rods versus cones, Wiley Interdisc. Rev. 1 (5) (2012) 675–683.
[2] G. Gestri, B.A. Link, S.C. Neuhauss, The visual system of zebrafish and its use to model human ocular diseases, Dev. Neurobiol. 72 (3) (2012) 302–327.
[3] M.C. Ciluffo, H.R. Matthews, S.E. Brockerhoff, G.L. Fain, Light-induced Ca^{2+} release in the visible cones of the zebrafish, Vis. Neurosci. 21 (2004) 599–609.
[4] Y.T. Leung, G.L. Fain, H.R. Matthews, Simultaneous measurements of current and calcium in the ultraviolet-sensitive cones of zebrafish, J. Physiol. 579 (1) (2007) 15–27.
[5] O. Rinner, Y.V. Makhankov, O. Biehlmaier, S.C.F. Neuhauss, Knockdown of cone-specific kinase GRK7 in larval zebrafish leads to impaired cone response recovery and delayed dark adaptation, Neuron 47 (2005) 231–242.
[6] F. Vogalis, T. Shiraki, D. Kojima, Y. Wada, Y. Nishiwaki, J.L.P. Jarvinen, J. Sugiyama, K. Kawakami, I. Masai, S. Kawamura, Y. Fukada, T.D. Lamb, Ectopic expression of cone-specific G-protein-coupled receptor kinase GRK7 in zebrafish rods leads to lower photosensitivity and altered responses, J. Physiol. 589 (2011) 2321–2348.
[7] G. Stearns, M. Evangelista, J.M. Fadool, S.E. Brockerhoff, A mutation in the cone-specific pde6 gene causes rapid cone photoreceptor degeneration in zebrafish, J. Neurosci. 27 (2007) 13866–13874.
[8] K. Palczewski, A. Polans, W. Baehr, J.B. Ames, Ca^{2+}-binding proteins in the retina: structure, function, and the etiology of human visual diseases, BioEssays 22 (2000) 337–350.
[9] K.W. Koch, T. Duda, R.K. Sharma, Ca^{2+}-modulated vision-linked ROS-GC guanylate cyclase transduction machinery, Mol. Cell. Biochem. 334 (2010) 105–115.
[10] Y. Imanishi, L. Yang, I. Sokal, S. Filipek, K. Palczewski, W. Baehr, Diversity of guanylate cyclase-activating proteins (GCAPS) in teleost fish: characterization of three novel GCAPs (GCAP4, GCAP5, GCAP7) from zebrafish (Danio rerio) and prediction of eight GCAPs (GCAP1-8) in pufferfish (Fugu rubripes), J. Mol. Evol. 59 (2) (2004) 204–217.
[11] N. Rätscho, A. Scholten, K.W. Koch, Expression profiles of three novel sensory guanylate cyclases and guanylate cyclase-activating proteins in the zebrafish retina, Biochim. Biopyhs. Acta 1793 (2009) 1110–1114.
[12] A. Scholten, K.W. Koch, Differential calcium signaling by cone specific guanylate cyclase-activating proteins from the zebrafish retina, PLoS ONE 6 (8) (2011) e23117.
[13] R. Fries, A. Scholten, W. Säftel, K.W. Koch, Operation profile of zebrafish guanylate cyclase-activating protein 3, J. Neurochem. 121 (2012) 54–65.
[14] K.A. Howes, M.E. Pennesi, I. Sokal, J. Church-Kopish, B. Schmidt, D. Margolis, J.M. Frederick, F. Rieke, K. Palczewski, S.M. Wu, P.B. Detwiler, W. Baehr, GCAP1 rescues rod photoreceptor response in GCAP1/GCAP2 knockout mice, EMBO J. 21 (7) (2002) 1545–1554.
[15] N.S. Peachey, S.L. Ball, Electrophysiological analysis of visual function in mutant mice, Doc. Ophthalmol. 107 (1) (2003) 13–36.
[16] B. Chang, N.L. Hawes, R.E. Hurd, M.T. Davisson, S. Nusinowitz, J.R. Heckenlively, Retinal degeneration mutants in the mouse, Vis. Res. 42 (4) (2002) 517–525.
[17] P.D. Calvert, N.V. Krasnoperova, A.L. Lyubarsky, T. Isayama, M. Nicolo, B. Kosaras, G. Wong, K.S. Gannon, R.F. Margolskee, R.L. Sidman, E.N. Pugh Jr., C.L. Makino, J. Lem, Phototransduction in transgenic mice after targeted deletion of the rod transducin alpha -subunit, Proc. Natl. Acad. Sci. U. S. A. 97 (25) (2000) 13913–13918.
[18] G.J. O'Sullivan, C.M. O'Tuathaigh, J.J. Clifford, G.F. O'Meara, D.T. Croke, J.L. Waddington, Potential and limitations of genetic manipulation in animals, Drug

Discov. Today Technol. 3 (2) (2006) 173–180.
[19] M. Aquila, M. Benedusi, A. Fasoli, G. Rispoli, Characterization of Zebrafish green cone Photoresponse recorded with pressure-polished patch pipettes, yielding efficient intracellular Dialysis, PLoS ONE 10 (10) (2015) e0141727.
[20] L.H. Cao, D.G. Luo, K.W. Yau, Light responses of primate and other mammalian cones, Proc. Natl. Acad. Sci. U. S. A. 111 (7) (2014) 2752–2757.
[21] M. Aquila, D. Dell' Orco, A. Fasoli, M. Benedusi, E. Kremmer, R. Fries, A.K.W. Scholten, G. Rispoli, Real-Time Modulation of Zebrafish Cone Phototransduction by Whole-Cell Delivery of zgcap3 and of its Monoclonal Antibody, Biophys. J. 104 2 (Suppl. 1) (2013) 103a.
[22] R. Fries, A. Scholten, W. Saftel, K.W. Koch, Zebrafish guanylate cyclase type 3 signaling in cone photoreceptors, PLoS ONE 8 (2013) e69656.
[23] D. Dell'Orco, P. Behnen, S. Linse, K.-W. Koch, Calcium binding, structural stability and guanylate cyclase activation in GCAP1 variants associated with human cone dystrophy, Cell. Mol. Life Sci. 67 (2010) 973–984, https://doi.org/10.1007/s00018-009-0243-8.
[24] P. Behnen, A. Scholten, N. Rätscho, K.W. Koch, The cone-specific calcium sensor guanylate cyclase activating protein 4 from the zebrafish retina, J. Biol. Inorg. Chem. 14 (2009) 89–99.
[25] M. Benedusi, M. Aquila, A. Milani, G. Rispoli, A pressure-polishing set-up to fabricate patch pipettes that seal on virtually any membrane, yielding low access resistance and efficient intracellular perfusion, Eur. Biophys. J. 40 (2011) 1215–1223.
[26] M. Aquila, M. Benedusi, A. Fasoli, G. Rispoli, Pressure-polished borosilicate pipettes are "universal sealer" yielding low access resistance and efficient intracellular perfusion, Methods Mol. Biol. 1183 (2014) 279–289.
[27] J.Y. Hwang, et al., Regulatory modes of rod outer segment membrane guanylate cyclase differ in catalytic efficiency and Ca(2+)-sensitivity, Eur. J. Biochem. 270 (2003) 3814–3821.
[28] N. Takemoto, S. Tachibanaki, S. Kawamura, High cGMP synthetic activity in carp cones, Proc. Natl. Acad. Sci. U. S. A. 106 (2009) 11788–11793.
[29] A. Moriondo, G. Rispoli, A step-by-step model of phototransduction cascade shows that Ca2+ regulation of guanylate cyclase accounts only for short-term changes of photoresponse, Photochem. Photobiol. Sci. 2 (12) (2003) 1292–1298.
[30] L. Lagnado, L. Cervetto, P.A. McNaughton, Calcium homeostasis in the outer segments of retinal rods from the tiger salamander, J. Physiol. 455 (1992) 111–142.
[31] S. Forti, A. Menini, G. Rispoli, V. Torre, Kinetics of phototransduction in retinal rods of the newt Triturus cristatus, J. Physiol. 419 (1989) 265–295.
[32] K.W. Koch, L. Stryer, Highly cooperative feedback control of retinal rod guanylate cyclase by calcium ions, Nature 334 (1988) 64–66.
[33] N. Ratscho, A. Scholten, K.W. Koch, Diversity of sensory guanylate cyclases in teleost fishes, Mol. Cell. Biochem. 334 (2010) 207–214.
[34] K. Sakurai, J. Chen, V.J. Kefalov, Role of guanylyl cyclase modulation in mouse cone phototransduction, J. Neurosci. 31 (2011) 7991–8000.
[35] A. Mendez, M.E. Burns, I. Sokal, A.M. Dizhoor, W. Baehr, K. Palczewski, D.A. Baylor, J. Chen, Role of guanylate cyclase-activating proteins (GCAPs) in setting the flash sensitivity of rod photoreceptors, Proc. Natl. Acad. Sci. U. S. A. 98 (2001) 9948–9953.
[36] M.E. Burns, A. Mendez, J. Chen, D.A. Baylor, Dynamics of cyclic GMP synthesis in retinal rods, Neuron 36 (2002) 81–91.
[37] M.L. Woodruff, A.P. Sampath, H.R. Matthews, N.V. Krasnoperova, J. Lem, G.L. Fain, Measurement of cytoplasmic calcium concentration in the rods of wild-type and transducin knock-out mice, J. Physiol. 542 (2002) 843–854.